

# Pulverization of Rubber Using Modified Solid State Shear Extrusion Process (SSSE)

Nima Shahidi, Hamid Arastoopour, George Ivanov

*Chemical and Environmental Engineering Department, Illinois Institute of Technology, Chicago, Illinois*

Received 1 August 2005; accepted 19 September 2005

DOI 10.1002/app.23259

Published online in Wiley InterScience (www.interscience.wiley.com).

**ABSTRACT:** The challenge of reusing scrap rubber material is mainly due to its crosslinked/vulcanized structure, which prevents the material from melting and from being melt processed into new items. The most feasible recycling approach is believed to be a process in which the vulcanized rubber is first pulverized into a fine powder and then incorporated into new products. Solid state shear extrusion (SSSE), developed at Illinois Institute of Technology, is a process for continuous pulverization of rubber materials into a fine powder (Arastoopour, H. U.S. Pat. 5,704,555 (1998); Arastoopour, H.; Schocke, D. A.; Bernstein, B.; Bilgili, E. U.S. Pat. 5,904,885 (1999); Ivanov, G. *Polym Eng Sci* 2000, 40, 676). In this work, the design of the SSSE apparatus was modified to overcome heat generation due to pulverization and the limitation from the torque/feeding rate relation and, thus, to increase the efficiency of the process in the production of finer particles at higher throughput. The modification was achieved by separating the original process into the extru-

sion section and the pulverization section. The extrusion section is dedicated to convey material to the pulverization section, which consists of a cylindrical housing and a rotatable cylindrical element that rotates independent of the extruder's screw. The rotatable cylindrical element can be treaded or flightless. Both sections are connected with an adapter. This new approach to the design allowed us to apply a more efficient cooling system, capable of removing the heat of pulverization and, in turn, results in the production of finer rubber particles. Furthermore, separation of the conveying process from the pulverization process resulted in a reduction in extruder's torque and a significant increase in the throughput. © 2006 Wiley Periodicals, Inc. *J Appl Polym Sci* 102: 119–127, 2006

**Key words:** rubber; recycling; pulverization; particle size distribution; degradation

## INTRODUCTION

Rubber recycling and production of high “value-added” materials from scrap rubber are challenging sustainability issues. Scrap tires represent the main stream of waste rubber materials that cannot be economically disposed of or efficiently reused using today's technology.<sup>1,2</sup> Although worldwide figures are imprecise, it is known that one-fourth of the 283 million tires scrapped in the United States wound up in landfills in 2003.<sup>3</sup> This figure is in addition to more than 300 million tires already stockpiled across the nation.<sup>3</sup> The main problem with recycling of rubber materials is the crosslinked structure of vulcanized rubber, which prevents their melting and further processing for reuse. The most feasible approach is the one in which rubber materials are first pulverized into fine particles and then incorporated into new rubber or plastic formulations.<sup>2,4,5</sup> Pulverization of rubber materials into fine particles is generally accomplished through the use of a cryogenic process, which is costly due to the use of liquid nitrogen.<sup>6–8</sup> Therefore, development of a cost-effective pulverization technology has been the subject of recent-year investigations.<sup>9,10–13</sup>

Solid state shear extrusion (SSSE) is an ambient pulverization process that is capable of producing fine rubber powder without the use of liquid nitrogen. This work is focused on a modified design of the SSSE process that results in a significant increase in the efficiency of the process in the production of fine rubber particles.<sup>14</sup> The original single screw extruder SSSE process was developed by Arastoopour and Ivanov in 1998.<sup>15,16</sup> The application of this technology to pulverization and recycling of rubber is shown by Arastoopour and coworkers,<sup>11</sup> based on the preliminary study of Schocke et al.<sup>13</sup> on the pulverization of rubber materials using a Bridgman anvil apparatus. Later, Bilgili et al.<sup>9,10</sup> demonstrated that the SSSE process produces a rubber powder, which has a higher surface area when compared with that produced by other pulverization processes. They observed a moderate level of degradation associated with the SSSE process and concluded that most of the chain breakages occur at the weak sulfur bonds, resulting in partial devulcanization of the rubber particles. The main challenge remaining in the SSSE process is the significant amount of heat generated during the process, which results in partial degradation and agglomeration of fine particles.<sup>9,10,17</sup> Heat generation is due to dissipation of elastic deformation energy into the form of heat energy.<sup>9</sup> Our goal is to provide a condition

Correspondence to: H. Arastoopour (arastoopour@iit.edu).

**TABLE I**  
**Approximate Weight Composition of the Rubber Granules Used in Pulverization Experiments Using the SSSE Apparatus**

Components	Per hundred resin (phr)	Weight percent (%)
Natural rubber	100	56.5
Zinc oxide	5	2.8
Stearic acid	6	3.4
SRF (carbon black)	41	23.2
TMQ (accelerator)	1	0.6
Wax	2	1.1
6 PPD (anti degradant)	2	1.1
Polyethylene	2	1.1
Aromatic oil	18	10.2

close to isothermal at the pulverization zone of the SSSE process with more efficient heat removal from the system. To achieve this goal, the original design of the SSSE process was divided into two separate portions; namely, the pulverization section and the extrusion section.<sup>14</sup> This modification enabled us to have better control of the processing conditions in the pulverization section of the SSSE apparatus.

## EXPERIMENTAL

### Materials

Rubber slabs specified as rubber Grade 6 were obtained from a company, with approximate composition as shown in Table I. The rubber slabs were cut into rectangular pieces so that they could be fed into a lab-scale Cumberland grinder to produce rubber granulates of smaller than 6 mm. The rubber granulates

produced were then sieved into two major size fractions of 2–4 mm and 4–6 mm. An equal amount of each size fractions was mixed using a tumble-blender for 15 min. The blended rubber granulates were used in the pulverization experiments with the SSSE apparatus.

### SSSE apparatus

The new design of the SSSE apparatus consists of an extrusion section and a pulverization section, as illustrated in Figure 1. As shown in this figure, within an elongated cylindrical housing, multicomponent screws are connected to each other, each having an extrusion portion and a pulverization portion. These two screws rotate independent of each other. The extrusion section of the SSSE process utilizes a commercially available laboratory scale C. W. Brabender single screw extruder. The pulverization section is custom-made.

The extrusion section of the SSSE process is capable of submitting a screw rotating speed ( $\omega_e$ ) of up to 100 rpm and delivering a maximum torque of 100 Nm. Three control thermocouples ( $T_{b1}$ ,  $T_{b2}$ , and  $T_{b3}$ ) are housed along the cylindrical barrel of the extrusion section. These thermocouples indicate the barrel wall temperature of the extruder. Three stock thermocouples ( $T_{m1}$ ,  $T_{m2}$ , and  $T_{m3}$ ) are also aligned flush with the rubber material to indicate the material temperature inside of the extruder. Three square-pitched screws with different geometries were used in the extrusion section as shown in Figure 2. All of these screws have a root diameter of 19.1 mm. The screw pitch, the flight thickness, and the flight angle at the root of each screw were 19.1 mm, 3.2 mm, and 17.4°, respectively. The channel depth at the

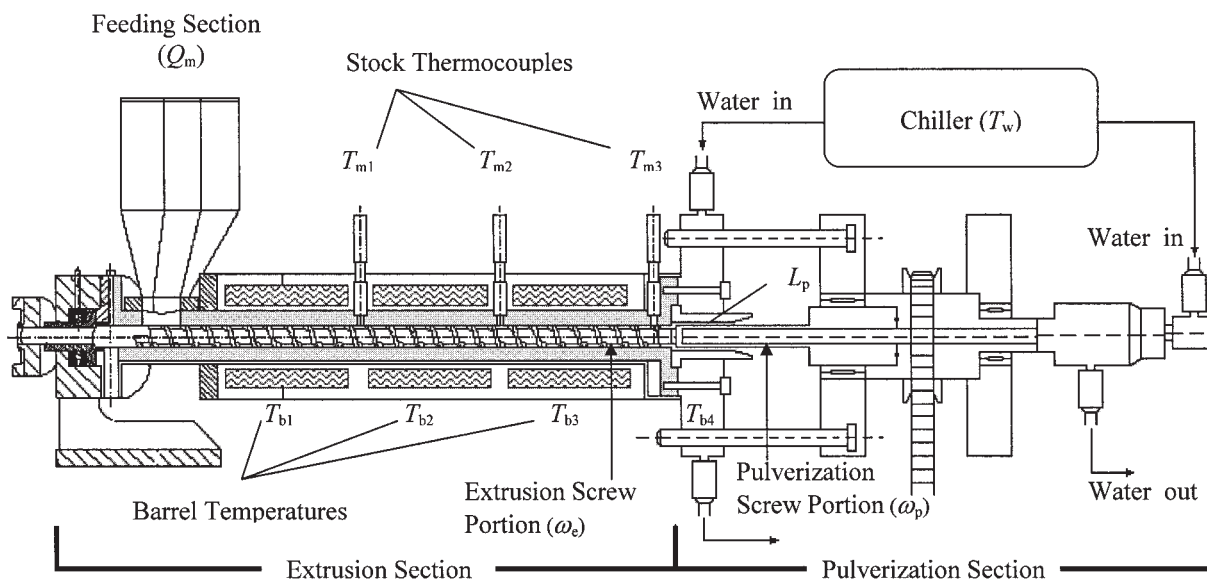


**Figure 1** A longitudinal schematic of the modified (new design) solid state shear. extrusion process.

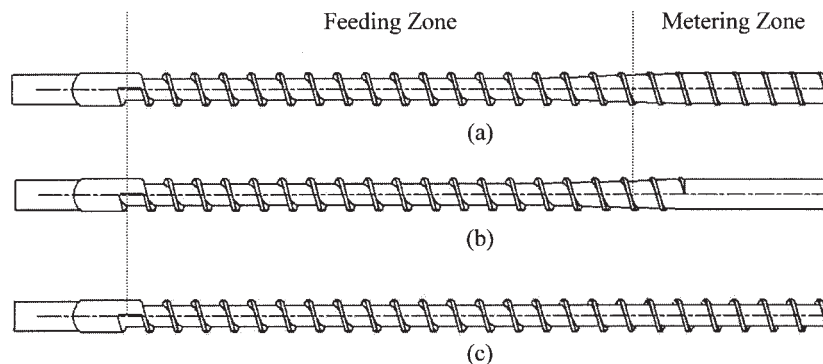


**Figure 2** Schematic of the screws used in the extrusion section of the SSSE process.

feeding zone of these screws is constant and equal to 3.8 mm. Two distinct sections can be defined for each screw; namely, the feeding zone and the metering zone (see Fig. 2). The feeding zone of the screw is limited to where the channel depth of the screw remains constant. The metering zone of the screw is located where the channel depth gradually decreases toward the end of screw. The metering zone has a major influence on regulating the output of the extruder. The ratio of the channel depth at the metering zone to the channel depth at the feeding zone identifies the compression ratio (CR) of screw. The first and second screws used in this work (see Fig. 2(a, b)) have a CR of 5 : 1 but a different flight design at their metering zone. The channel depth at the metering zone of these screws is 0.76 mm. These two screws were used in the original design of the SSSE apparatus that utilizes only the extrusion section of the apparatus shown in Figure 1. The third screw (see Fig. 2(c)) has a CR of one, which indicates that the channel depth at the end of screw is the same as the depth of the channel at the initial point of the screw (3.8 mm). This means that the extruder was used as a screw feeding device. The screw with a CR of one does not apply any compressive force on the materials. Bilgili et al.<sup>9</sup> found that only a screw with a CR greater than one is capable of applying the necessary compressive shear force on the material for significant pulverization. Therefore, it is expected that no pulverization will occur using a screw with a CR of one. In the new SSSE design, the screw with a CR of one was used in the extrusion section to minimize the pulverization of rubber granulates in this section. The aim was to provide a controlled condition at lower temperature for pulverization in the pulverization section only.

In the pulverization section, the rubber granulates pass through a gap between the inner surface of an elongated cylindrical housing ( $L_p$ ) and the outer surface of the pulverization screw portion. Controllable shear and compression forces can be applied on the rubber granulates in this section by manipulating the rotation speed of the pulverization screw portion ( $\omega_p$ ) and the gap between the cylindrical housing and the screw. The electrical motor of the pulverization section

is capable of submitting a rotating speed of up to 150 rpm. A circulating water-cooling system (Thermonslab M100) was used to maintain the temperature of the pulverization section ( $T_{b4}$ ) at a low temperature. The temperature controlling system provided in the pulverization section in the new design comprises an inner cooling tube within the pulverization screw portion along with a cooling jacket surrounding the pulverization cylindrical housing. The pulverization screw portion is flightless and the gap between the screw and the housing is such that a “compression ratio” of 5 : 1 is maintained. The screw that is used in the extrusion section has a compression ratio of 1 (see Fig. 2(c)).

Pulverization of rubber granulates was performed at different processing conditions as shown in Table II. The rubber granulates were fed at a maximum rate into the feeding zone of the extrusion section ( $Q_m$ ).

The original design of the SSSE apparatus, which utilizes only the extrusion section of the apparatus (shown in Fig. 1), was used to study the effect of screw design on the size distribution of the resulting particles. In this case, the third zone of the extrusion section ( $T_{b3}$ ), where most of the pulverization is expected to occur,<sup>9,18</sup> has to be equipped with a water-cooling jacket. Two screws with different designs (see Fig. 2(a, b)) were used in this case study (Test runs SE-01 and SE-02). Using the new SSSE design, the effects of cooling water temperature, rotation speed of the pulverization screw portion, and length of the elongated cylindrical housing on the size distribution of the particles were studied (test runs SEP-03 to SEP-09).

### Particle size characterization

Approximately 200 g of the rubber particles produced in each experiment was collected. The powder samples were cooled to room temperature in a desiccator prior to particle size characterization. The rubber particles were dry-sieved using steel US standard test sieves manufactured by W. S. Tyler. The particle size

**TABLE II**  
Operating Conditions of the SSSE Process in the Pulverization Experiments

Test no.	SSSE design	$L_p$ (mm)	$T_{b1}, T_{b2}$ (°C)	$T_{b3}$ (°C)	$T_w$ (°C)	$\omega_e$ (rpm)	$\omega_p$ (rpm)
SE-01	Original <sup>a</sup>	100 <sup>b</sup>	80	40	25	80	–
SE-02	Original <sup>c</sup>	100 <sup>b</sup>	80	40	25	80	–
SEP-03	New	46	80	80	5	35	150
SEP-04	New	46	80	80	20	35	150
SEP-05	New <sup>d</sup>	46	80	80	20	35	150
SEP-06	New	28.5	80	80	20	35	150
SEP-07	New	76	80	80	20	35	150
SEP-08	New	46	80	80	20	35	50
SEP-09	New	46	80	80	20	35	100

<sup>a</sup> The screw with flights was used in this experiment (see Fig. 2 (a)).

<sup>c</sup> The flightless screw was used in this experiment (see Fig. 2 (b)).

<sup>d</sup> Cooling water was injected only into the barrel wall of the pulverization section.

<sup>b</sup> The length of the pulverization barrel in the original SSSE is located in the extruder section.

measurements were repeated 3 times for each experiment run and the procedure was conducted according to the standard test method defined in the annual publication of the American Society for Testing and Materials (ASTM).<sup>19</sup> The particles were separated into a number of different size fractions, which were subsequently weighed. The result is a mass distribution of the equivalent mesh diameter. In the sieving method, determination of the distribution function is reasonably accurate because of the use of a comparatively large quantity of particles. The reproducibility of this technique depends upon the quality of the separation and possible attrition of the particles during vibration of the sieves. The volume mean diameter,  $d_{vm}$ , and Sauter mean diameter,  $d_{\text{versus}}$ , of the particles produced were calculated using sieve data.  $d_{vm}$  is sensitive to the presence of coarser particles in the powder, whereas  $d_{\text{versus}}$  is sensitive to the presence of finer particles. The mass geometric mean diameter,  $d_{gm}$ , and geometric standard deviation,  $\delta_g$ , of the powder were determined using the following equation:

$$\log d_{gm} = \frac{\sum_i (\log d_i \times \Delta\phi_i)}{100} \quad (1)$$

$$\ln \delta_g = \left( \frac{\sum_i \{[\ln(d_i/d_{gm})]^2 \times \Delta\phi_i\}}{100} \right)^{1/2} \quad (2)$$

where  $d_i$  and  $\Delta\phi_i$  represent diameter and mass fraction of size  $i$  particles.

### Thermal characterization

Thermogravimetric analysis (TGA) and differential thermogravimetry (DTG) were performed to determine the thermal degradation behavior of the sam-

ples. This characterization technique was performed to investigate the degree of degradation of rubber particles during the SSSE process. A thermogravimetric analyzer, Polymer Laboratories STA 625, was used for this purpose. Experiments were conducted in the temperature range of 35–550°C under a purge of nitrogen gas at a scanning rate of 10°C/min. Samples were prepared in open pans containing about 10 mg of sample.

## RESULTS AND DISCUSSION

### Effect of screw design

The effect of screw design was determined by measuring the particle size distribution of the pulverized rubber using the original design of the SSSE process. This study was performed using the screws marked (a) and (b) in Figure 2. Using the original design, most of the pulverization occurs at the metering zone of the

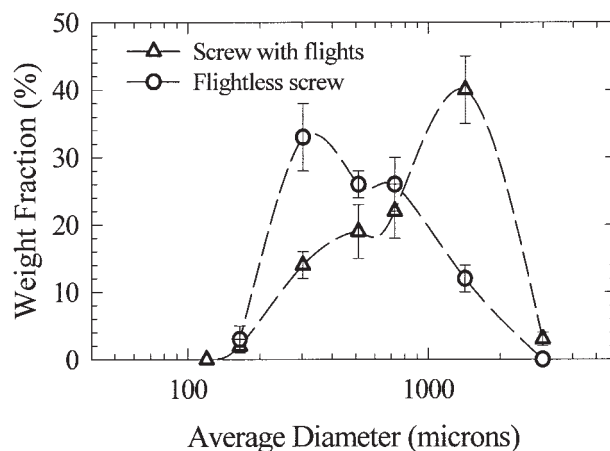


**Figure 3** Differential particle size distributions using screws with different flight designs (Runs SE-01 and SE-02).

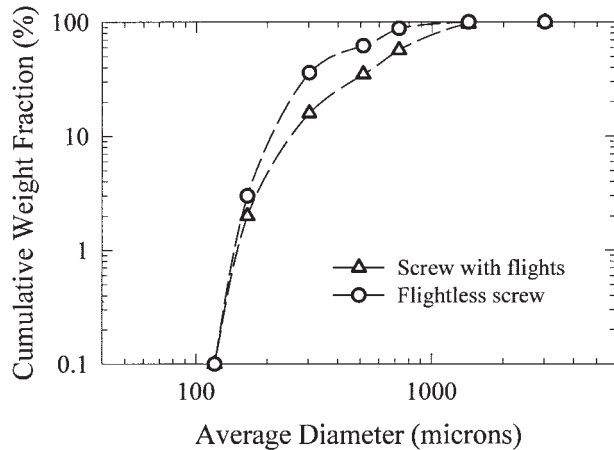


**Figure 4** Cumulative particle size distributions using screws with different flight designs (Runs SE-01 and SE-02).

screw ( $L_p = 100$  mm), where the rubber granulates are subjected to maximum compressive and shear forces because of reduction in channel depth of the rotating screw. It is essential to maintain a low temperature at the third zone ( $T_{b3}$ ) of the extruder for removing the heat of pulverization and to minimize stress relaxation of rubber molecules. The operating conditions are given in Table II as test no. SE-01 and SE-02. The particle size distribution of the powder produced using these two screws is shown in Figures 3 and 4. It was observed that the screw without flights at its metering zone produced finer particles when compared with those produced by the screw with flights. The  $d_{vm}$  and  $d_{versus}$  of the produced particles were determined at  $963 \mu\text{m}$  and  $646 \mu\text{m}$  for the screw with flights, and  $598 \mu\text{m}$  and  $450 \mu\text{m}$  for the screw without flights (see Table III). This can be explained such that when the rubber particles reach the metering zone of the flightless screw, they start to accumulate at this point. As a result, higher residence time and finer particles could be obtained using the flightless screw when compared with those obtained using the screw with flights. The residence time of the material in the

extrusion section was measured to be approximately at 32 and 102 s for the screw with and without flights, respectively. Higher compression force due to accumulation of the particles in the flightless screw resulted in pulverization of the rubber to smaller particles. Additionally, accumulation of the particles at the flightless zone of the screw increases the residence time of the particles at this zone. If a screw with flights conducts single breakage of particles, then the flightless screw with much higher residence time most likely provides multiple breakages of the particles. It is important to note that higher residence time of the rubber particles at the pulverization zone also results in significant heat generation and subsequently, agglomeration of the particles. To better remove heat from the pulverized particles, the pulverization section was separated from the extruder section in our new design.

#### Cooling efficiency in the new SSSE design

To investigate the efficiency of the heat removal and its effect on pulverization, low temperature water ( $T_w$ ) was introduced into the cooling system of the pulverization section (Tests SEP-03, and SEP-04). The results were compared with the case of introducing cooling water only into the barrel cooling jacket of the pulverization section without cooling the screw portion (Test SEP-05). These experiments were performed at  $T_w$  of 5 and  $20^\circ\text{C}$ , while all the other processing parameters were kept constant. The particle size distribution of the pulverized rubber at these processing conditions was measured 3 times (see Figs. 5 and 6 for average particle size). As shown in these figures, bimodal distributions were observed, similar to those results previously obtained by Bilgili et al.<sup>9</sup> When cooling water at 5 and  $20^\circ\text{C}$  was introduced into both the screw and the cylindrical housing cooling jacket of the pulverization section, the particle size distributions of the produced particles shifted toward smaller particles. However, when cooling water was introduced only into the cylindrical housing cooling jacket of the pul-

**TABLE III**  
Effects of Processing Conditions on Dependent Variables

Test no.	$d_{vm}$ ( $\mu\text{m}$ )	$d_{vs}$ ( $\mu\text{m}$ )	$d_{gm}$ ( $\mu\text{m}$ )	$\delta_g$	$T_{m2}$ ( $^\circ\text{C}$ )	$T_{m3}$ ( $^\circ\text{C}$ )	$T_{b4}$ ( $^\circ\text{C}$ )	$T_{app}$ ( $^\circ\text{C}$ )	$Q_m$ (g/min)
SE-01	963	646	284	2.90	65	45	–	52	4.6
SE-02	598	450	195	2.71	80	58	–	68	4.6
SEP-03	1008	470	270	2.86	40	68	40	44	20.9
SEP-04	1047	559	284	2.89	40	72	49	50	20.9
SEP-05	1298	672	349	2.99	42	82	58	58	20.9
SEP-06	1650	873	438	3.11	40	73	45	52	20.9
SEP-07	465	258	146	2.54	41	74	50	53	20.9
SEP-08	1195	420	762	2.85	40	88	58	58	20.9
SEP-09	1180	558	310	2.90	46	77	49	49	20.9

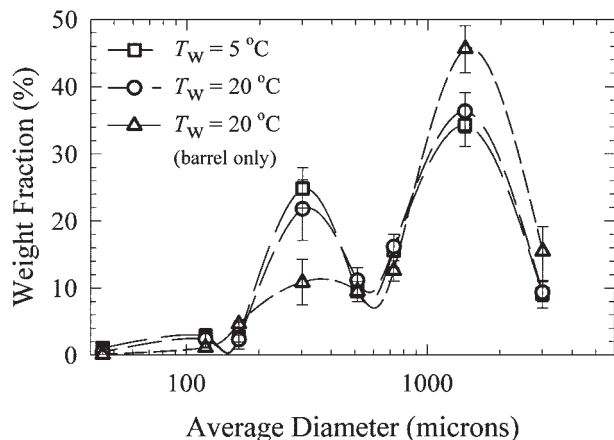


**Figure 5** Effect of cooling water temperature on differential particle size distribution (Runs SEP-03, SEP-04, and SEP-05).

verization section, the distribution curves shifted towards larger particles. This suggests that pulverization occurs both at the interface of the rubber with the cylindrical housing and the screw when they are both cooled with water. In the case of introducing cooling water only into the cylindrical housing cooling jacket, the temperature of the pulverization screw portion increased (see Test no. SEP-05 in Table III). Because of the stress relaxation effect of rubber at its interface with the screw having a high temperature, pulverization occurred only at the interface of the rubber with the cylindrical housing cooling jacket, resulting in production of larger particles.

Table III shows a lower value of  $\delta_g$  and thus narrower particle size for the produced rubber particles using cooling water in both the screw and cylindrical housing cooling jacket of the pulverization zone (SEP-03 and SEP-04) when compared with those ob-

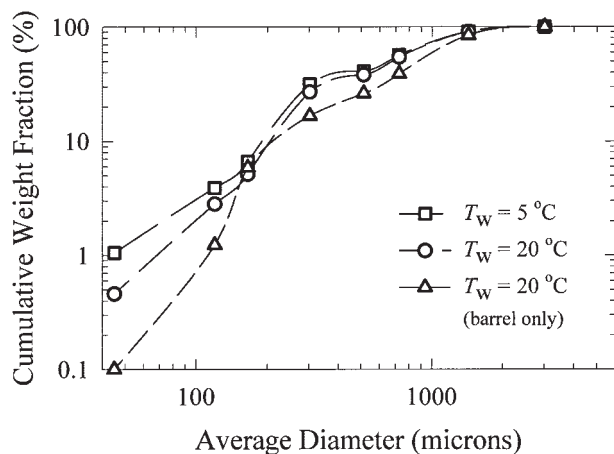


**Figure 6** Effect of cooling water temperature on cumulative particle size distribution (Runs SEP-03, SEP-04, and SEP-05).

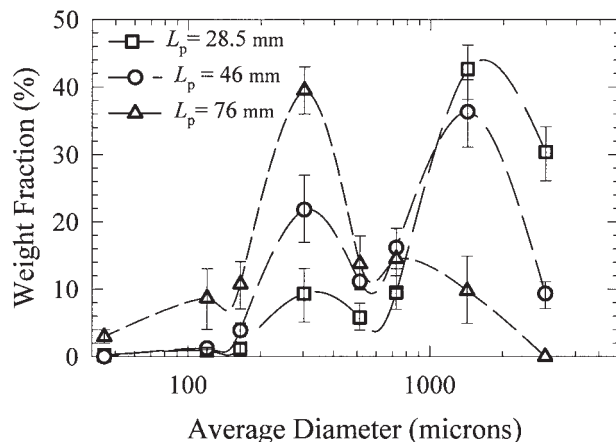


**Figure 7** Effect of pulverization zone length on particle size distribution (Runs SEP-06, SEP-07, and SEP-04).

tained in test no. SEP-05. Lowering the temperature and minimizing the temperature variation at a sufficiently long pulverization zone result in smaller particle size (see SEP07 in which  $d_{vm}$  and  $d_{versus}$  of the produced particles were at 465 and 258  $\mu\text{m}$ , respectively). Our experimental results showed that the heat removal from the pulverized rubber particles was more efficient by cooling both the cylindrical housing and screw portions of the pulverization section. These modifications can potentially decrease the agglomeration and degradation of the produced rubber particles.

#### Effect of length of the pulverization cylindrical housing

Three pulverization housing sections with lengths ( $L_p$ ) of 28.5, 46, and 76 mm were used to determine the effect of the length and residence time on the pulverization of rubber. The size distribution of the resulting pulverized particles is shown in Figures 7 and 8. For the case of the pulverization lengths of 28.5 and 46 mm, bimodal distributions with a higher particle concentration peak at the larger particle sizes were obtained. For the case of 76 mm pulverization housing, the higher particle concentration peak was obtained at a smaller size. In a shorter pulverization zone, the residence time of the particles at the pulverization zone is probably not sufficient for pulverization into fine particles. It is expected that a single pulverization step of the particles will be dominant for the short pulverization zone case. Using a longer pulverization zone, the residence time of the particles at that zone is longer. Thus, multiple pulverization steps of the materials most likely occur, resulting in a shift in the size distribution of the particles of smaller sizes.

It is important to note that the apparent temperature of the pulverized rubber did not change significantly,

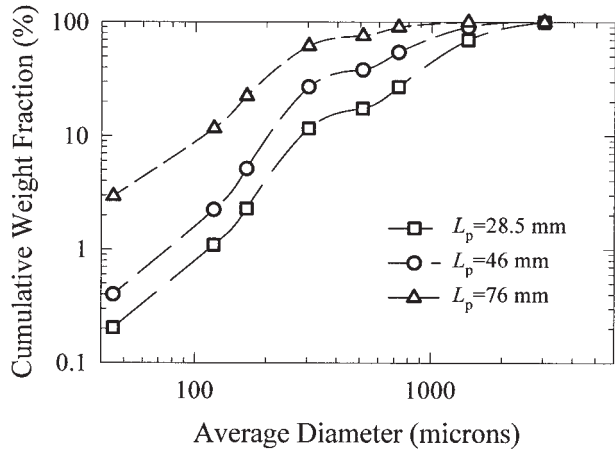


**Figure 8** Effect of pulverization zone length on cumulative particle size distribution (Runs SEP-06, SEP-07, and SEP-04).

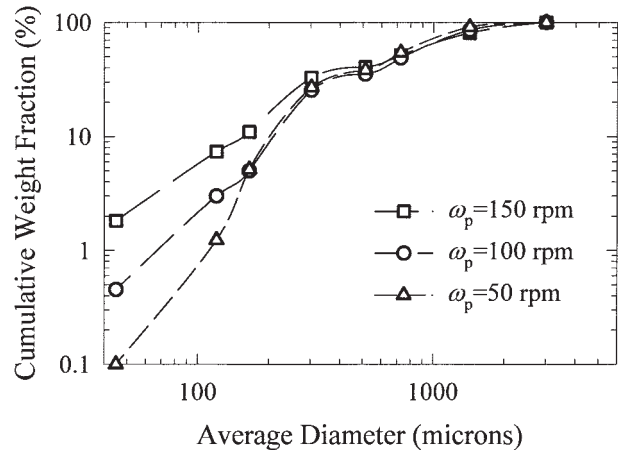


**Figure 10** Effect of pulverization screw speed on the cumulative particle size distribution (Runs SEP-06, SEP-07, and SEP-04).

although the residence time of the particles was expected to be longer in the 76 mm pulverization housing setup when compared with that in the 28.5 mm housing. This result indicates the high efficiency of the new SSSE design for removing heat from the system. Table III shows that the  $\delta_{gr}$ ,  $d_{vm}$ , and  $d_{versus}$  of the produced particles all decrease with increased length of the pulverization zone. This means that smaller particles with a narrow size distribution may be produced under the condition of more uniform and lower temperature, using the optimum length for the pulverization zone.

**Effect of rotation speed of the pulverization screw**

To determine the effect of rotation speed of the screw at the pulverization section,  $\omega_p$  was changed while  $\omega_e$  was kept constant at 35 rpm. Figures 9 and 10 show the size distribution of the pulverized particles resulting from tests SEP-08, SEP-09, and SEP-04 conducted

at  $\omega_p$  of 50, 100, and 150 rpm. Figures 9 and 10 show production of smaller particles with narrower size distribution by increasing the rpm. This result might be due to higher shear strain deformation of the rubber particles at higher rotation speeds that lead to pulverization into finer and more uniform particles. At the lowest rotational speed of 50 rpm, the material temperature was higher due to the higher frictional heat dissipation at the pulverization zone. This suggests that the stored elastic energy due to large deformation was dissipated in the form of heat rather than surface energy change by pulverization into finer particles.<sup>13</sup>

**Comparing the original and new SSSE designs**

The main advantage of the new design is a significant increase in throughput of the SSSE process and at the same time production of finer particles. As indicated in Table III, the maximum attainable throughput of the original design of the SSSE is about 4.6 g/min. In the new design, the throughput of the SSSE process is increased to 20.9 g/min; (almost four times). This is the maximum flow rate of the laboratory scale extruder used in this work. The effect of processing conditions in the new SSSE design was determined by measuring the size distribution of the resulting particles. Figures 11 and 12 show the comparison of the typical particle size distribution of the rubber powder produced by the new and original design of the SSSE process at their optimum processing condition (Runs SE-02 and SEP-07). The  $d_{vm}$  and  $d_{versus}$  of the resulting powder in these two runs (see Table III) indicate that a finer powder can be produced using the new design of the SSSE apparatus. The  $T_{app}$  value of the pulverized rubber was measured at 68°C using the original design of the SSSE apparatus, while this value was

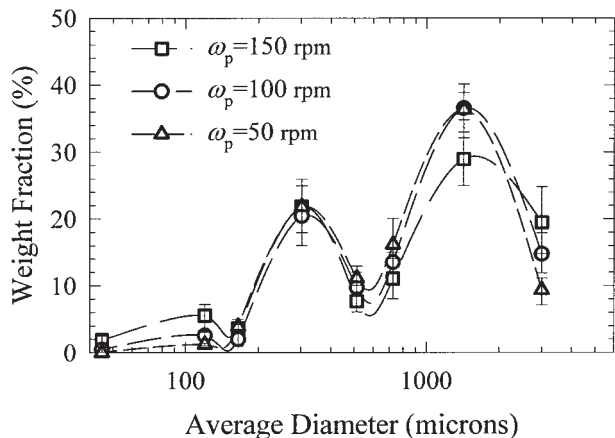


**Figure 9** Effect of pulverization screw speed on particle size distribution (Run SEP-06, SEP-07, and SEP-04).

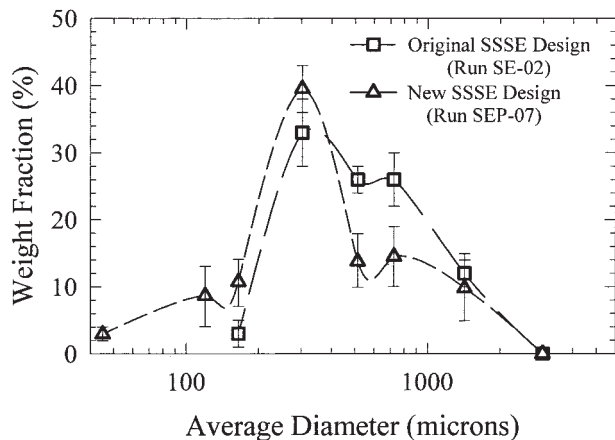


**Figure 11** Comparison between optimum particle size distribution of the rubber particles produced based on our experimental data using the original and new SSSE designs (Runs SE-02 and SEP-07).

measured at 53°C in the new design. This result indicates that the heat generation due to pulverization of rubber can be removed more efficiently from the rubber particles in our new design. This leads to a lower degree of agglomeration and degradation of the rubber particles during the process. Figure 12 shows that no particle of less than 100  $\mu\text{m}$  was produced using the old design, while more than 10% of the rubber particles smaller than 100  $\mu\text{m}$  were produced using the new design of the SSSE apparatus. Furthermore, particles produced using the new design have a narrow size distribution. This means that there is a higher efficiency of the new SSSE design in producing finer particles with narrower size distribution.

### Thermal degradation behavior

The TGA and DTG traces of the rubber powder produced under processing conditions of test SEP-04 are

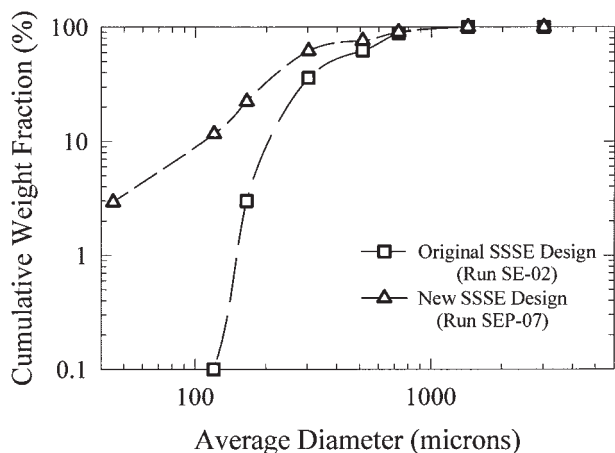


**Figure 12** Comparison between cumulative optimum particle size distribution of the rubber particles produced based on our experimental data using original with new SSSE designs (Runs SE-02 and SEP-07).

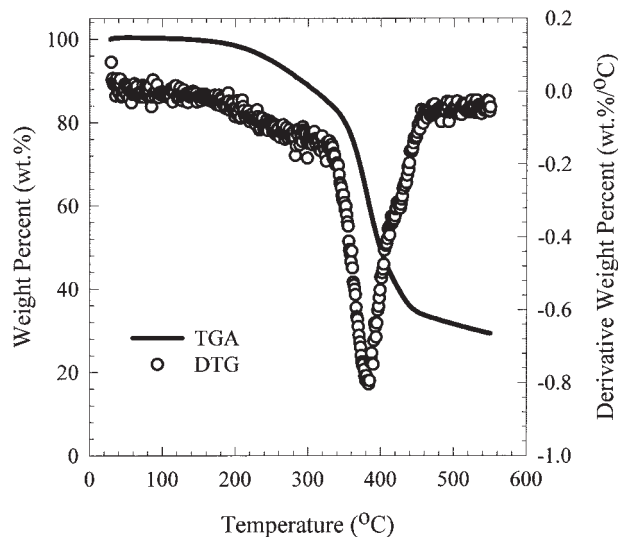


**Figure 13** TGA and DTG traces of the pulverized rubber particles.

presented in Figure 13. Two weight losses were observed during the experiment. The first weight loss occurred in the temperature range of 200–300°C, and the second weight loss occurred in the temperature range of 300–440°C. The major weight loss observed in the temperature range of 300–440°C is expected to be due to thermal degradation of the natural rubber.

Carbon black is the main additive used in the rubber compound (see Table I). Carbon black and some inorganic additives remain in the form of residues at temperatures above 450°C in a nitrogen environment. As indicated in Table I, a small portion of the rubber compound consists of organic substances that are expected to degrade in the temperature range of 200–

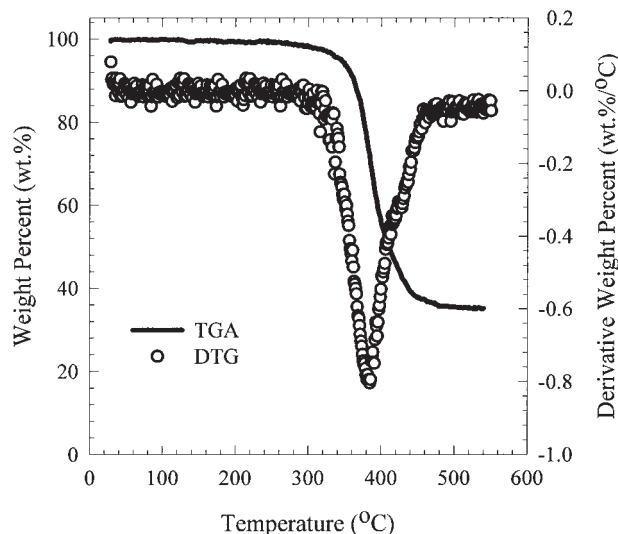


**Figure 14** TGA and DTG traces of the gel fraction of the pulverized rubber particles.



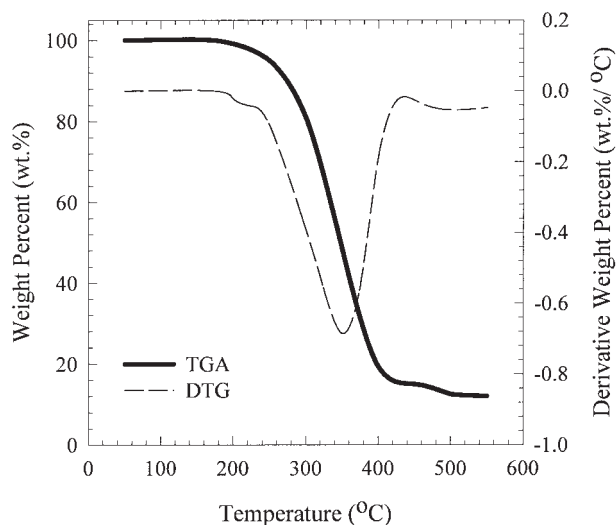


**Figure 15** TGA and DTG traces of the sol fraction of the pulverized rubber particles.

300°C. The weight loss observed at this temperature range might be due to degradation of the organic oil used in the compounding step, or the short rubber chains formed during the SSSE process due to chain scission. Both the organic oil and the short rubber chains can be extracted from the particles using the Soxhlet extraction technique.<sup>19</sup> Using this extraction technique, the rubber particles can be divided into two portions, namely the gel fraction and the sol fraction. The gel fraction is the insoluble portion in the fluid carrier (toluene) used and the sol fraction is the soluble portion that is expected to be composed of organic oil and short rubber chains.

Figure 14 shows the TGA and DTG traces of the gel fraction after drying it in a vacuum oven at 60°C for 12 h. As shown in this figure, only one weight loss was observed that could be related to the degradation of crosslinked rubber. This is based on inspection of DTG traces of the original sample shown in Figure 13, indicating that the extent of degradation at 380°C is similar to that obtained in the original sample. After extraction, the weight loss in the temperature range of 200–300°C that was observed in the unextracted rubber particles disappeared. This is due to extraction of low molecular weight substances from the particles. The chemical nature of the extracted materials (sol fraction) was characterized by performing thermal characterization, as shown in Figure 15. In this figure, it can be observed that a majority of the extracted substances was actually low molecular weight rubber chains as the weight loss occurred in the temperature range of 300–440°C. To investigate the degree of rub-

ber degradation in the SSSE process, the extraction procedure was performed on the rubber granulates prior to pulverization and compared with the results obtained on the pulverized rubber. The total amount of extracted material from the rubber particles after pulverization was found to be 8 wt %. The extraction experiment on the rubber granulates prior to the pulverization process indicated that this amount is about 6 wt %. This finding suggests that the chain scission of rubber molecules during the SSSE process is negligible. Thus, it can be concluded that the degree of rubber degradation during the SSSE process is not significant.

## CONCLUSIONS

A lower and more uniform temperature was provided at the pulverization zone of the SSSE process by separating the pulverization section from the extrusion section in the original design of the SSSE process. Using the new design, finer rubber particles with narrower particle size distribution were obtained at higher throughput when compared with the original design of the SSSE process. It was observed that residence time of the particles in the SSSE process has a major influence on the size of the produced particles. By maintaining a screw inner cooling system, the heat removal from the system was enhanced, resulting in a lower degree of degradation.

## References

1. Fang, Y.; Zhan, M.; Wang, Y. *Mater Des* 2001, 22, 123.
2. Blumenthal, M. Presented at the 163th Rubber Division Meeting of ACS, Pittsburgh, PA, October 2002.
3. Recycling Research Institute, *The Scrap Tire and Rubber Users Directory* 2003; Recycling Research Institute, 2003.
4. Burford, R. P.; Pittolo, M. *J Mater Sci* 1986, 21, 2308.
5. Pittolo, M.; Burford, R. P. *J Mater Sci* 1986, 21, 1769.
6. Rouse, M.W. *Rubber World* 1992, 205, 25.
7. Dierkes, W. *Rubber World* 1996, 214, 25.
8. Leyden, J. *Rubber World* 1991, 203, 28.
9. Bilgili, E.; Arastoopour, H.; Bernstein, B. *Powder Technol* 2001, 115, 265.
10. Bilgili, E.; Arastoopour, H.; Bernstein, B. *Powder Technol* 2001, 115, 277.
11. Arastoopour, H.; Schocke, D. A.; Bernstein, B.; Bilgili, E. U.S. Pat. 5,904,885 (1999).
12. Khait, K. *Rubber World* 1997, 216, 38.
13. Schocke, D.; Arastoopour, H.; Bernstein, B. *Powder Technol* 1999, 102, 207.
14. Ivanov, G. K.; Arastoopour, H.; Bilgili, E.; Shahidi, N.; Bernstein, B. U.S. Pat. 6,513,737 (2003).
15. Arastoopour, H. U.S. Pat. 5,704,555 (1998).
16. Ivanov, G. US Pat. 5,743,471 (1998).
17. Wolfson, S. F.; Nikolskii, V. A. *Polym Eng Sci* 1997, 37, 1294.
18. Ivanov, G. *Polym Eng Sci* 2000, 40, 676.
19. Annual Book of ASTM Standards. ASTM D 5644-01.